IEEE Access
Multidisciplinary | Rapid Review | Open Access Journal

Date of publication xxxx 00, 0000, date of current version xxxx 00, 0000.

Digital Object Identifier 10.1109/ACCESS.2020.Doi Number

A Multiplicative Noises and Additive Correlated Noises Cubature Kalman Filter and its Application in Quadruped Robot

Jikai Liu[1], Pengfei Wang[1], Mantian Li[1], Wei Guo[1], Fusheng Zha[1,2], Lining Sun[1], and Penglong Zheng[1]

[1] State Key Laboratory of Robotics and System, Harbin Institute of Technology, Harbin 150080, China

[2] Shenzhen Academy of Aerospace Technology, Shenzhen 518057, China

Corresponding authors: Fusheng Zha (e-mail: zhafusheng@hit.edu.cn); Lining Sun (e-mail: 15806215871@139.com).

This work was supported by Natural Science Foundation of China (No.61773139), The Foundation for Innovative Research Groups of the National Natural Science Foundation of China (Grant No.51521003), Shenzhen Science and Technology Program (No.KQTD2016112515134654) and Shenzhen Science and Technology Research and Development Foundation (No.JCYJ20190813171009236).

ABSTRACT The traditional Cubature Kalman Filter (CKF) and its derived algorithms cannot work without the two hypotheses of Kalman Filter (KF), one is that the system model is accurate and the other is the system is only influenced by independent white noise with known statistical characteristics. However, it is difficult to fully guarantee the above hypotheses in actual operation. The presence of multiplicative noise undermines the first hypothesis, while the additive noise correlation undermines the second hypothesis. Given invalid hypotheses, the estimated performances of CKF and its derivative algorithms are degraded drastically. To solve this issue, this paper proposes Multiplicative Noises and Additive Correlated Noises Cubature Kalman Filter (MACNCKF), which solves state estimation problems involving multiplicative noise and additive noise while maintaining CKF advantages. Moreover, this algorithm has been testified to be correct and easy to be transplanted to CKF and its derivative algorithm after strict mathematical derivation. When the system lacks multiplicative noise and additive noise, the algorithm is degraded to corresponding algorithm in a general form, which helps extend the application environment of CKF and its derivative algorithms, thus improving robustness. Numerical simulation and experiments on quadruped robot system indicate that MACNCKF can effectively solve state estimation problem involving both multiplicative noise and additive noise. Given time consumption in MACNCKF basically comparable to that in CKF, MACNCKF has improved estimation accuracy, robustness and reliability.

INDEX TERMS Quadruped Robot; State Estimation; MACNCKF; IMU; Kinematics.

I. INTRODUCTION

A key aspect of robotics today is estimating the state, such as position and orientation, of a robot as it moves through the world. Most robots and autonomous vehicles depend on noisy data from sensors such as cameras or laser rangefinders to navigate in a three-dimensional world [1]. A sensor has limited accuracy, even the best sensor has a certain degree of uncertainty, which thus raises the problem of state estimation. An important approach for state estimation is to establish a system mathematical model with random disturbances for related problems, and then make an optimal estimation of the system state variable based on the model. When establishing a mathematical model of an system, random interference is usually viewed as an additive noise. For example, classical Kalman Filter (KF) theory is modeled in this way. However, in many application fields, actual systems are often complex and changeable, which is impossible to be described by pure linear models. Such systems are generally known as non-linear systems. Estimation algorithms are generally based on several improved forms of the KF algorithm, such as Extended Kalman Filter (EKF) [2], Unscented Kalman Filter (UKF) [3], and Cubature Kalman Filter (CKF) [4]. Therefore, it can be said that these multi-sensor fusion algorithms developed from KF theory default to two hypotheses of KF theory: the system model is accurate; the system is only affected by mutually independent white noise with known statistical characteristics. Moreover, to guarantee convenient algorithm design, it is usually assumed that the system's process noise and observation

This article has been accepted for publication in a future issue of this journal, but has not been fully edited. Content may change prior to final publication. Citation information: DOI 10.1109/ACCESS.2020.3021494, IEEE Access

noise are additive noise independent of each other. These are quite ideal hypotheses about parameter accuracy and noise characteristics in the system model for the sake of convenient construction of the filtering algorithm. The state estimation performance of the designed nonlinear filtering algorithm can only be guaranteed when the assumed ideal conditions are met. However, in practical applications, mathematical models are approximated, and the existence of bias is always inevitable. Due to approximation of the model degree, linear approximation of the nonlinear system, and errors brought by parameter identification, there is a certain error between the acquired mathematical model and the actual system. Moreover, due to changes in the surrounding environment and presence of several unpredictable disturbances, the system model has the above-mentioned uncertainties. It can be seen that the two hypotheses of KF theory are quite ideal, which can hardly be met in the actual system. In the fields such image information processing [5], pattern recognition [6], underwater target tracking [7], aircraft tracking [8], space target tracking [9], and robot state estimation [10], there exists another type of non-ideal circumstances that in the process of signal transmission, there will be delay, distortion, attenuation or channel interference, the random uncertainty of system model parameters will be caused by modeling error, model simplification and random disturbance, the ranging noise of the sensor varies with the increase of the distance and appears as multiplicity noise [11]. These circumstances cannot be indicated by additive noise in classical systems. If the actual disturbance is ignored in use of fusion algorithm on the basis of ideal hypothesis, the derived fusion result may be very unsatisfactory. Hence, multiplicative noise systems can characterize a wider range of practical systems.

In spite of this fact, as it is difficult to determine the statistical characteristics of observation noise and dynamic noise, many researchers assume system noise and observation noise as independent white noise. The current fusion estimation methods for integrated navigation and positioning mainly focus on fusion positioning under hypotheses of independent noise and related noise. However, independence between measurement noise and system noise represents an ideal hypothesis. For practical systems, sensors affected by the working environment are often prone to interference sources, making the system and the sensor jointly influenced by relevant noise in the working process. This is manifested as the correlation between process noise and observation noise in description of the system model, and will be affected by uncertain factors.

In recent years, state estimation algorithms under non-ideal conditions are deeply concerned by relevant researchers. Fruitful research results have been achieved and linear filtering algorithms under non-ideal conditions have well developed [12-18]. The main idea is to construct pseudo state equation. Redefinition of process noise is no longer formally related to existing observation noise, but there are few non-linear filtering algorithms under non-ideal conditions. Chang G [19] studied noise-related processing approaches under the existing nonlinear filtering algorithm framework, and its main idea was similar to the method in [12-18], representing application of such idea in non-linear filtering algorithms. In addition, Chang G also pointed out that process noise has correlation with observation noise, so the former's conditional probability density against the latter is greater than the former's own probability density, which means that the state accuracy derived based on conditional probability density is higher. Moreover, a method was proposed to deal with synchronization-related noise by using the properties of conditional Gaussian distribution. However, the results are only applicable to linear Kalman filtering algorithm framework. Simon D [20] took an aircraft control system model as an example to illustrate that process noise has correlation with observation noise in the system model under the influence of random gusts. Saha S [21] used conditional distribution to modify the proposal distribution in the algorithm under the condition of noise synchronization, which was similar to the processing method in [20]. For the issue of multiplicative noise, Hu [11] proposed Generalized Kalman Filter (GKF), which used definitions of mean, covariance, and cross-covariance for mathematical derivation, and improved calculation equation for estimates and variance of measured updated state variables in the KF framework. Wang [22] proposed a KF + ML filtering method by combining maximum likelihood estimation (ML) and KF. Basin [23] approximated the system to a polynomial form and proposed a root mean square filter. The above researches on non-linear filtering algorithms under non-ideal conditions only focus on one of the non-ideal conditions, that is, either multiplicative noise or additive noise correlation. As far as we know, there is no non-linear filtering algorithm considering both multiplicative noise and correlated noise. Therefore, to avoid the two ideal hypotheses of KF at the same time and make the nonlinear filtering algorithm more applicable to practical situations, this paper proposes a Multiplicative Noises and Additive Correlated Noises Cubature Kalman Filter (MACNCKF) based on CKF with the best comprehensive performance. The algorithm can solve nonlinear system state estimation problem involving both multiplicative noise and correlated noise , which cannot only be easily transplanted into the third-degree, fifth-degree, seventh-degree, and mixed-order CKF without the restriction of the sampling strategy of CKF algorithm, but also applied to CKF using square root for iteration free from the limitation of iterative strategy.

After simulation and experiments on a quadruped robot platform, it is testified that the algorithm can effectively solve state estimation problem of non-linear systems with both multiplicative noise and synchronous additive noise. With real-time performance comparable to CKF, its computation complexity is not greatly increased, which fully meets real-time requirements. Moreover, the estimation accuracy is greatly improved compared with CKF, which verifies the correctness and effectiveness of MACNCKF.

This article has been accepted for publication in a future issue of this journal, but has not been fully edited. Content may change prior to final publication. Citation information: DOI 10.1109/ACCESS.2020.3021494, IEEE Access

II. MULTIPLICATIVE NOISES AND ADDITIVE CORRELATED NOISES CUBATURE KALMAN FILTER

The standard CKF does not take into account multiplicative noise, process noise and observation noise in the system equation. Based on CKF, this section proposes an improved CKF algorithm to solve the problems related to multiplicative noise, process noise and observation noise. The following nonlinear system with multiplicative and additive noise is considered:

$$x_{k+1} = M_k f\left(x_k, u_k\right) + w_k \tag{1}$$

$$z_k = N_k h\left(x_k, u_k\right) + v_k \tag{2}$$

Where, $x_{k+1} \in R^a$ is the system state vector at the moment $k+1$, $z_k \in R^b$ is the system observation vector at the moment k; $f(\cdot)$ and $h(\cdot)$ are respectively state equation and observation equation of the time-varying system. $w_k \in R^a$ is the system process noise, $v_k \in R^b$ is the system observation noise, which are synchronously related zero-mean Gaussian white noise, and $E = \left\{ \begin{bmatrix} w_k \\ v_k \end{bmatrix} \begin{bmatrix} w_k^T & v_k^T \end{bmatrix} \right\} = \begin{bmatrix} Q_k & C_k \\ C_k^T & R_k \end{bmatrix} \delta_{kl}$. Q_k is the process noise variance, R_k is the observation noise variance, C_k is the covariance between the two, δ_{kl} represents the Kronecker function. Generally, the random parameter disturbance is Gaussian white noise with zero mean, then there is Gaussian white noise $M_k = diag\left[1+m(k), ..., 1+m(k)\right]_{a\times a}$ with mean m and variance σ_m^2; Gaussian white noise $N_k = diag\left[1+n(k), ..., 1+n(k)\right]_{b\times b}$ with mean n and variance σ_n^2.

The standard CKF algorithm is detailed in [4], which will not be further described here due to space limitations. Similarly, the improved MACNCKF algorithm consists of two steps: time prediction and observation update. Since this algorithm is commonly used in CKF and its various derivative algorithms, to avoid loss of generality, the sampling strategy and iterative strategy are not discussed here. The specific expression of MACNCKF is as follows:

A. TIME PREDICTION

Given the estimated value $\hat{x}_{k-1/k-1}$ and the covariance matrix $P_{k-1/k-1}$ of the state variable at the moment $k-1$, the posterior covariance matrix $P_{zz,k-1/k-1}$ of the observation quantity is calculated accordingly, then the one-step prediction estimate and one-step prediction covariance matrix of the state variable x_k at the moment k can be calculated accordingly:

$$\begin{aligned} P_{zz,k-1/k-1} &= \left(1+2n+n^2\right) Var\left\{h\left(x_{k-1}\right)\right\} + R_{k-1} + \dots \\ &\quad \sigma_n^2 \left(Var\left\{h\left(x_{k-1}\right)\right\} + E\left\{h\left(x_{k-1}\right)\right\} E\left\{h^T\left(x_{k-1}\right)\right\}\right) \end{aligned} \tag{3}$$

$$\begin{aligned} \hat{x}_{k/k-1} &= C_{k-1} P_{zz,k-1/k-1}^{-1} \left(z_{k-1} - N_{k-1} h\left(\hat{x}_{k-1/k-1}\right)\right) + \dots \\ &\quad (1+m) \int f\left(x_{k-1}\right) \boldsymbol{N}\left(x_{k-1}; \hat{x}_{k-1/k-1}, P_{k-1/k-1}\right) dx_{k-1} \end{aligned} \tag{4}$$

$$\begin{aligned} P_{k/k-1} &= Q_{k-1} - C_{k-1} P_{zz,k-1/k-1}^{-1} C_{k-1}^T + \dots \\ &\quad \left(1+2m+m^2\right) Var\left\{f\left(x_{k-1}\right)\right\} + \dots \\ &\quad \sigma_m^2 \left(Var\left\{f\left(x_{k-1}\right)\right\} + E\left\{f\left(x_{k-1}\right)\right\} E\left\{f^T\left(x_{k-1}\right)\right\}\right) \end{aligned} \tag{5}$$

Where, $\boldsymbol{N}\left(x; \hat{x}, P\right)$ indicates Gaussian probability density function of the variable x.

B. OBSERVATION UPDATE

$$\hat{z}_{k/k-1} = (1+n) \int h\left(x_k\right) \boldsymbol{N}\left(x_k; \hat{x}_{k/k-1}, P_{k/k-1}\right) dx_k \tag{6}$$

$$\begin{aligned} P_{zz,k/k-1} &= \left(1+2n+n^2\right) Var\left\{h\left(x_k\right)\right\} + R_k + \dots \\ &\quad \sigma_n^2 \left(Var\left\{h\left(x_k\right)\right\} + E\left\{h\left(x_k\right)\right\} E\left\{h^T\left(x_k\right)\right\}\right) \\ P_{xz,k/k-1} &= \sigma_*^2 \left(\beta+\gamma\right) + (1+m)(1+n)\delta \end{aligned} \tag{7}$$

where

$$\begin{aligned} \beta &= \operatorname{cov}\left\{f\left(x_{k-1}\right), h\left(x_k\right)\right\} \\ \gamma &= E\left\{f\left(x_{k-1}\right)\right\} E\left\{h^T\left(x_k\right)\right\} \\ \delta &= \operatorname{cov}\left\{f\left(x_{k-1}\right), h\left(x_k\right)\right\} \end{aligned} \tag{8}$$

$$K_k = P_{xz,k/k-1} P_{zz,k/k-1}^{-1} \tag{9}$$

$$\hat{x}_{k/k} = \hat{x}_{k/k-1} + K_k \left(z_k - \hat{z}_{k/k-1}\right) \tag{10}$$

$$P_{k/k} = P_{k/k-1} - K_k P_{zz,k/k-1} K_k^T \tag{11}$$

Demonstration:

$$\begin{aligned} P_{zz,k-1/k-1} &= E\left\{\left(z_{k-1} - \hat{z}_{k-1/k-1}\right)\left(z_{k-1} - \hat{z}_{k-1/k-1}\right)^T \middle| D_{k-1}\right\} \\ &= (1+n)^2 Var\left\{h\left(x_{k-1}\right)\right\} + R_{k-1} + \dots \\ &\quad \left(E\left\{n^2(k-1)\right\} - n^2\right) E\left\{h\left(x_{k-1}\right) h^T\left(x_{k-1}\right) \middle| D_{k-1}\right\} \\ &= \left(1+2n+n^2\right) Var\left\{h\left(x_{k-1}\right)\right\} + R_{k-1} + \dots \\ &\quad \sigma_n^2 \left(Var\left\{h\left(x_{k-1}\right)\right\} + E\left\{h\left(x_{k-1}\right)\right\} E\left\{h^T\left(x_{k-1}\right)\right\}\right) \end{aligned} \tag{12}$$

Equation (3) is proved.

$$\begin{aligned} \hat{x}_{k/k-1} &= E\left\{x_k \middle| D_{k-1}\right\} \\ &= E\left\{M_{k-1} f\left(x_{k-1}\right) \middle| D_{k-1}\right\} + E\left\{w_{k-1} \middle| D_{k-1}\right\} \end{aligned} \tag{13}$$

It can be known from Lemma [2] that

$$\begin{Bmatrix} w_{k-1} \middle| \hat{x}_{k-1/k-1} \\ z_{k-1} \middle| \hat{x}_{k-1/k-1} \end{Bmatrix} \sim \boldsymbol{N}\left(\begin{pmatrix} 0 \\ N_{k-1} h\left(\hat{x}_{k-1/k-1}\right) \end{pmatrix}, \begin{bmatrix} Q_{k-1} & C_{k-1} \\ C_{k-1}^T & P_{zz,k-1/k-1} \end{bmatrix}\right) \tag{14}$$

The conditional probability density of the noise w_{k-1} with respect to the observation z_{k-1} is

$$\begin{aligned} &P\left(w_{k-1} \middle| \hat{x}_{k-1}, z_{k-1}\right) = \boldsymbol{N}\left(\sigma, Q_{k-1} - C_{k-1} P_{zz,k-1}^{-1} C_{k-1}^T\right) \\ &\textit{where} \\ &\sigma = C_{k-1} P_{zz,k-1}^{-1} \left(z_{k-1} - N_{k-1} h\left(\hat{x}_{k-1}\right)\right) \end{aligned} \tag{15}$$

Since w_{k-1} is irrelevant with observation sequence D_{k-2}, then

This article has been accepted for publication in a future issue of this journal, but has not been fully edited. Content may change prior to final publication. Citation information: DOI 10.1109/ACCESS.2020.3021494, IEEE Access

$$P\left(w_{k-1}\left|\hat{x}_{k-1/k-1},z_{k-1}\right.\right)=P\left(w_{k-1}\left|\hat{x}_{k-1/k-1},D_{k-1}\right.\right) \tag{16}$$

That is,

$$E\left\{w_{k-1}\left|D_{k-1}\right.\right\}=C_{k-1}P_{zz,k-1/k-1}^{-1}\left(z_{k-1}-N_{k-1}h\left(\hat{x}_{k-1/k-1}\right)\right) \tag{17}$$

$$E\left\{w_{k-1}w_{k-1}^{T}\left|D_{k-1}\right.\right\}=Q_{k-1}-C_{k-1}P_{zz,k-1/k-1}^{-1}C_{k-1}^{T} \tag{18}$$

$$\begin{aligned}\hat{x}_{k/k-1}&=C_{k-1}P_{zz,k-1/k-1}^{-1}\left(z_{k-1}-N_{k-1}h\left(\hat{x}_{k-1/k-1}\right)\right)+\ldots\\&\left(1+m\right)\int f\left(x_{k-1}\right)\boldsymbol{N}\left(x_{k-1};\hat{x}_{k-1/k-1},P_{k-1/k-1}\right)dx_{k-1}\end{aligned} \tag{19}$$

Equation (4) is proved.

$$\begin{aligned}P_{k/k-1}&=E\left\{\left(x_k-\hat{x}_{k/k-1}\right)\left(x_k-\hat{x}_{k/k-1}\right)^{T}\left|D_{k-1}\right.\right\}\\&=\sigma_m^2\left(Var\left\{f\left(x_{k-1}\right)\right\}+E\left\{f\left(x_{k-1}\right)\right\}E\left\{f^{T}\left(x_{k-1}\right)\right\}\right)+\ldots\\&\left(1+2m+m^2\right)Var\left\{f\left(x_{k-1}\right)\right\}+\ldots\\&Q_{k-1}-C_{k-1}P_{zz,k-1/k-1}^{-1}C_{k-1}^{T}\end{aligned} \tag{20}$$

Since the observation noise variance is $E\left\{v_{k-1}v_{k-1}^{T}\left|D_{k-1}\right.\right\}=Q_{k-1}-C_{k-1}P_{zz,k-1/k-1}^{-1}C_{k-1}^{T}$, equation (5) is proved.

Measurement update

$$\begin{aligned}\hat{z}_{k/k-1}&=E\left\{N_kh\left(x_k\right)+V_k\left|D_{k-1}\right.\right\}\\&=\left(1+n\right)\int h\left(x_k\right)\boldsymbol{N}\left(x_k;\hat{x}_{k/k-1},P_{k/k-1}\right)dx_k\end{aligned} \tag{21}$$

Equation (6) is proved.

$$\begin{aligned}P_{xz,k/k-1}&=E\left\{\left(x_k-\hat{x}_{k/k-1}\right)\left(z_k-\hat{z}_{k/k-1}\right)^{T}\left|D_{k-1}\right.\right\}\\&=\left(1+m\right)\left(1+n\right)\mathrm{cov}\left\{f\left(x_{k-1}\right),h\left(x_k\right)\right\}+\ldots\\&\left(E\left\{m\left(k-1\right)n\left(k\right)\right\}-mn\right)E\left\{f\left(x_{k-1}\right)h^{T}\left(x_k\right)\left|D_{k-1}\right.\right\}\\&=\left(1+m\right)\left(1+n\right)\mathrm{cov}\left\{f\left(x_{k-1}\right),h\left(x_k\right)\right\}+\ldots\\&\sigma_*^2\left(\mathrm{cov}\left\{f\left(x_{k-1}\right),h\left(x_k\right)\right\}+E\left\{f\left(x_{k-1}\right)\right\}E\left\{h^{T}\left(x_k\right)\right\}\right)\end{aligned} \tag{22}$$

If the two multiplicative noises are independent of each other, the cross covariance is $\sigma_*^2=0$, Equation (7) is proved.

$$\begin{aligned}P_{zz,k/k-1}&=E\left\{\left(z_k-\hat{z}_{k/k-1}\right)\left(z_k-\hat{z}_{k/k-1}\right)^{T}\left|D_{k-1}\right.\right\}\\&=\left(1+2n+n^2\right)Var\left\{h\left(x_k\right)\right\}+R_k+\ldots\\&\sigma_n^2\left(Var\left\{h\left(x_k\right)\right\}+E\left\{h\left(x_k\right)\right\}E\left\{h^{T}\left(x_k\right)\right\}\right)\end{aligned} \tag{23}$$

Equation (8) is proved.

Substitute equations (4)~(8) into equations (9)~(11), it can be seen that when the system has no multiplicative noise, that is, $m=n=\sigma_m^2=\sigma_n^2=0$, and the process noise is not synchronized with the observation noise, that is, $\sigma_*^2=0$, MACNCKF degrades to the standard CKF, thus preliminarily verifying rationality of the algorithm design.

C. MACNCKF IMPLEMENTATION BASED ON MSSRCKF

The MACNCKF algorithm is commonly used in CKF and its various derivative algorithms. This section provides a discretized approximation algorithm flow based on Mixed-degree Spherical Simplex-Radial Cubature Kalman Filter (MSSRCKF) [24]. MSSRCKF is a CKF algorithm adopting mixed-order simplest phase-path sampling strategy. In sampling, $2n+3$ volume points are collected based on 3th-order surface integral and 5th-order radial integration, which has only 3 more volume points than the standard CKF, but the accuracy approaches to that of 5th-order CKF [25]. If the third-, fifth-, seventh-, or other-order CKFs are used, their steps are similar to MACNCKF steps based on MSSRCKF, with the only difference being the number and weights of volume points. Therefore, there will be no repetitions here, and collocation at will is possible according to actual needs. Square root of the state posterior covariance is used in the iteration. SVD decomposition or Cholesky decomposition can be performed, but for stability consideration, SVD decomposition is a decomposition method applicable to any matrix, with computation complexity equivalent to that of Cholesky decomposition. However, error in filtering process due to non-positive definiteness of the one-step prediction mean square error matrix is avoided after multiple loops, which improves robustness of the numerical calculation and also improves accuracy of the filtering. Therefore, SVD decomposition is adopted when calculating the volume points. If other iterative strategies are used, their steps are similar, which will not be repeated here. The steps of MACNCKF implementation based on MSSRCKF are given as follows:

1) INITIALIZATION

Suppose that the state estimation $\hat{x}_{k-1}$ and state variance matrix P_{k-1} at the moment $k-1$ are known, then according to the simplest phase-path sampling rule:

Take a set of vectors $a_i=[a_{i,1},a_{i,2},...,a_{i,n}]^T$,i=1,2,…n+1, where n is the state dimension.

$$a_{i,j}=\begin{cases}-\left[\dfrac{n+1}{n(n-j+2)(n-j+1)}\right]^{0.5}, & j<i\\0, & j>i\\\left[\dfrac{(n+1)(n-i+1)}{n(n-i+2)}\right]^{0.5}, & j=i\end{cases} \tag{24}$$

The volume point of the filter is expressed as:

$$\begin{cases}\xi_i=0, & i=0\\\xi_i=[\sqrt{(n+2)}a]_i, & i=1,2,...,n+1\\\xi_i=-[\sqrt{(n+2)}a]_i, & i=n+2,...,2n+2\end{cases} \tag{25}$$

Where, $[\ ]_i$ represents the calculated n dimensional point set, the number of points is $n+1$, and the weight corresponding to the volume point is:

$$\begin{cases}\omega_i=\dfrac{2}{n+2}, & i=0\\\omega_i=\dfrac{n}{2(n+1)(n+2)}, & i=1,2,...,2n+2\end{cases} \tag{26}$$

2) TIME UPDATE

Perform SVD decomposition of the state variance P_{k-1} at the moment $k-1$:

$$P_{k-1/k-1}=U_{k-1/k-1}S_{k-1/k-1}V_{k-1/k-1}^{T} \tag{27}$$

This article has been accepted for publication in a future issue of this journal, but has not been fully edited. Content may change prior to final publication. Citation information: DOI 10.1109/ACCESS.2020.3021494, IEEE Access

Where, $S_{k-1}=diag\left(s_1,s_2,...,s_r,0,...,0\right),s_1>s_2>\ldots>s_r>0$ is the singular value of the matrix P_{k-1}; $U_{k-1},S_{k-1},V_{k-1}\in R^{n\times n}$.

First, there is need to calculate ξ_i according to equations (24) and (25), and perform the first volume point calculation:

$$\chi_{i,k-1/k-1}=U_{k-1/k-1}\sqrt{S_{k-1/k-1}}\xi_i+\hat{x}_{k-1/k-1},i=0,1,...2n+2 \quad (28)$$

Volume point propagation:

$$\chi^*_{i,k/k-1}=f\left(\chi_{i,k-1/k-1},u_{k-1}\right),i=0,1,...,2n+2 \quad (29)$$

$$Z_{i,k-1/k-1}=h\left(\chi_{i,k-1/k-1},u_{k-1}\right) \quad (30)$$

Calculate the posterior observation estimate without multiplicative noise at the moment $k-1$:

$$\tilde{z}_{k-1/k-1}=h\left(\hat{x}_{k-1/k-1},u_{k-1}\right) \quad (31)$$

Calculate the posterior observation variance estimate at the moment $k-1$:

$$P_{zz,k-1/k-1}=\left(1+2n+n^2\right)a+R_{k-1}+\sigma_n^2\left(b+c\right)$$

where

$$a=\left(\sum_{i=0}^{2n+2}\omega_i Z_{i,k-1/k-1}Z^T_{i,k-1/k-1}-\tilde{z}_{k-1/k-1}\tilde{z}^T_{k-1/k-1}\right) \quad (32)$$

$$b=\sum_{i=0}^{2n+2}\omega_i Z_{i,k-1/k-1}Z^T_{i,k-1/k-1}-\tilde{z}_{k-1/k-1}\tilde{z}^T_{k-1/k-1}$$

$$c=\sum_{i=0}^{2n+2}\omega_i Z_{i,k-1/k-1}\cdot\sum_{i=0}^{2n+2}\omega_i Z^T_{i,k-1/k-1}$$

Calculate one-step prediction estimate of state variables without multiplicative noise at the moment k:

$$\tilde{x}_{k/k-1}=\sum_{i=0}^{2n+0}\omega_i\chi^*_{i,k/k-1}+C_{k-1}P^{-1}_{zz,k-1/k-1}\left(z_{k-1}-\tilde{z}_{k-1/k-1}\right) \quad (33)$$

Calculate one-step prediction estimate of state variables without multiplicative noise at the moment k:

Calculate one-step prediction estimate of the state variable at the moment k:

$$\hat{x}_{k/k-1}=\left(1+m\right)\sum_{i=0}^{2n+2}\omega_i\chi^*_{i,k/k-1}+C_{k-1}P^{-1}_{zz,k-1/k-1}\left(z_{k-1}-\tilde{z}_{k-1/k-1}\right) \quad (34)$$

Calculate one-step prediction estimate of the state variable variance at the moment k:

$$P_{k/k-1}=\left(1+2m+m^2\right)a+\sigma_m^2\left(b+c\right)+d$$

where

$$a=\left(\sum_{i=0}^{2n+2}\omega_i\chi^*_{i,k/k-1}\chi^{*T}_{i,k/k-1}-\tilde{x}_{k/k-1}\tilde{x}^T_{k/k-1}\right)$$

$$b=\sum_{i=0}^{2n+2}\omega_i\chi^*_{i,k/k-1}\chi^{*T}_{i,k/k-1}-\tilde{x}_{k/k-1}\tilde{x}^T_{k/k-1} \quad (35)$$

$$c=\sum_{i=0}^{2n+2}\omega_i\chi^*_{i,k/k-1}\cdot\sum_{i=0}^{2n+2}\omega_i\chi^{*T}_{i,k/k-1}$$

$$d=Q_{k-1}-C_{k-1}P^{-1}_{zz,k-1/k-1}C^T_{k-1}$$

3) OBSERVATION UPDATE

Perform SVD decomposition on the one-step prediction $P_{k/k-1}$ of the state variable variance at the moment k:

$$P_{k/k-1}=U_{k/k-1}S_{k/k-1}V^T_{k/k-1} \quad (36)$$

Second volume point calculation

$$\chi_{i,k/k-1}=U_{k/k-1}\sqrt{S_{k/k-1}}\xi_i+\hat{x}_{k/k-1},i=0,1,...,2n+2 \quad (37)$$

Second volume point propagation

$$Z_{i,k/k-1}=h\left(\chi_{i,k/k-1},u_k\right),i=0,1,...,2n+2 \quad (38)$$

Calculate one-step prediction estimate of observed variable without multiplicative noise at the moment k:

$$\tilde{z}_{k/k-1}=\sum_{i=0}^{2n+2}\omega_i Z_{i,k/k-1} \quad (39)$$

Calculate one-step prediction estimate of observed variable at the moment k:

$$\hat{z}_{k/k-1}=\left(1+n\right)\sum_{i=0}^{2n+2}\omega_i Z_{i,k/k-1} \quad (40)$$

Calculate one-step prediction estimate of the covariance at the moment k:

$$P_{xz,k/k-1}=\left(1+m\right)\left(1+n\right)a+\sigma_*^2\left(b+c\right)$$

where

$$a=\left(\sum_{i=0}^{2n+2}\omega_i\chi_{i,k/k-1}Z^T_{i,k/k-1}-\tilde{x}_{k/k-1}\tilde{z}^T_{k/k-1}\right) \quad (41)$$

$$b=\sum_{i=0}^{2n+2}\omega_i\chi_{i,k/k-1}Z^T_{i,k/k-1}-\tilde{x}_{k/k-1}\tilde{z}^T_{k/k-1}$$

$$c=\sum_{i=0}^{2n+2}\omega_i\chi^*_{i,k/k-1}\cdot\sum_{i=0}^{2n+2}\omega_i Z^T_{i,k/k-1}$$

If the two multiplicative noises are uncorrelated, then $\sigma_*^2=0$.

Calculate one-step prediction estimate of observed variance at the moment k:

$$P_{zz,k/k-1}=\left(1+2n+n^2\right)a+R_k+\sigma_n^2\left(b+\right)$$

where

$$a=\left(\sum_{i=0}^{2n+2}\omega_i Z_{i,k/k-1}Z^T_{i,k/k-1}-\tilde{z}_{k/k-1}\tilde{z}^T_{k/k-1}\right) \quad (42)$$

$$b=\sum_{i=0}^{2n+2}\omega_i Z_{i,k/k-1}Z^T_{i,k/k-1}-\tilde{z}_{k/k-1}\tilde{z}^T_{k/k-1}$$

$$c=\sum_{i=0}^{2n+2}\omega_i Z_{i,k/k-1}\cdot\sum_{i=0}^{2n+2}\omega_i Z^T_{i,k/k-1}$$

Calculate the state estimate and variance estimate at the moment k:

$$K_k=P_{xz,k/k-1}P^{-1}_{zz,k/k-1} \quad (43)$$

$$\hat{x}_{k/k}=\hat{x}_{k/k-1}+K_k\left(z_k-\hat{z}_{k/k-1}\right) \quad (44)$$

$$P_{k/k}=P_{k/k-1}-K_kP_{zz,k/k-1}K^T_k \quad (45)$$

4) NUMERICAL EXPERIMENTS

To verify and analyze feasibility of the MACNCKF algorithm proposed herein, the state equation (1) and observation equation (2) are simulated.

$$x_{k+1}=M_kFx_k+w_k \quad (46)$$

This article has been accepted for publication in a future issue of this journal, but has not been fully edited. Content may change prior to final publication. Citation information: DOI 10.1109/ACCESS.2020.3021494, IEEE Access

$$z_k = N_k\left(Hx_k + U\right) + v_k \tag{47}$$

$$F = \begin{bmatrix} 1 & 0 & T & 0 & T^2/2 & 0 \\ 0 & 1 & 0 & T & 0 & T^2/2 \\ 0 & 0 & 1 & 0 & T & 0 \\ 0 & 0 & 0 & 1 & 0 & T \\ 0 & 0 & 0 & 0 & 1 & 0 \\ 0 & 0 & 0 & 0 & 0 & 1 \end{bmatrix}, \tag{48}$$

$$H = \begin{bmatrix} 1 & 0 & 0 & 0 & 0 & 0 \\ 0 & 1 & 0 & 0 & 0 & 0 \\ 0 & 0 & 1 & 0 & 0 & 0 \\ 0 & 0 & 0 & 1 & 0 & 0 \end{bmatrix}, U = \begin{bmatrix} 0.015 \\ 0.015 \\ 0.14 \\ 0.001 \end{bmatrix}$$

State variables $x_k = \begin{bmatrix} x_k & y_k & \dot{x}_k & \dot{y}_k & \ddot{x}_k & \ddot{y}_k \end{bmatrix}^T$; x_k, $\dot{x}_k$, $\ddot{x}_k$ respectively represent the position, velocity and acceleration on the coordinate axis x. y_k, $\dot{y}_k$, $\ddot{y}_k$ respectively represent the position, velocity and acceleration on the coordinate axis y. The multiplicative noise matrixes M_k and N_k are randomly generated according to the definition, w_k and v_k are randomly generated Gaussian white noise. The sampling time is set to $T = 0.005s$, $Q_k = [0.125, 0, 0.25, 0; 0, 0.125, 0, 0.25; 0.25, 0, 0.5, 0; 0, 0.25, 0, 0.5]$, R_k is eye(4), the initial state is $x_0 = [3;\ 3;\ 0;\ 0;\ 0.5;\ 0]$, and P_0 is eye (4). $m = -9.9312\times10^{-4}$, $n = 2.2258\times10^{-4}$, $\sigma_m^2 = 9.8014\times10^{-4}$, $\sigma_n^2 = 1.0021\times10^{-4}$, $\sigma_*^2 = -1.6\times10^{-3}$, $C_k = 0.4896$. In the simulation, the Root Mean Square Error (RMSE) is used as the comparison standard. Suppose that sampling interval is $T = 0.005s$ and the number of Monte Carlo simulation times is 50. Figure 1 shows the northeast trajectory of simulation object in Monte Carlo simulation.

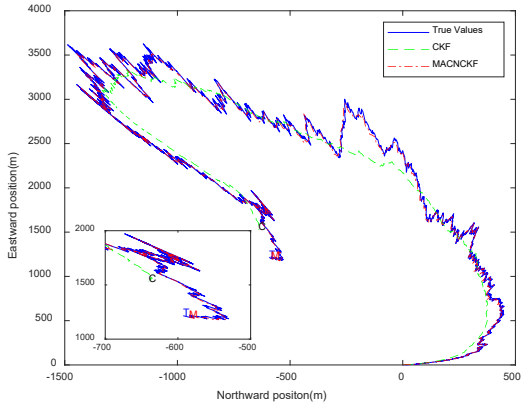

FIGURE 1. Moving trajectory of simulation object in one Monte Carlo run.

Figure 1 shows the North-East moving trajectory of simulation object in Monte Carlo simulation, where the solid line stands for the real position moving track, the dotted line denotes the position moving track estimated by CKF, and the dot dash line denotes the position moving track estimated by MACNCKF. In the experiment, there are multiplicative Gaussian white noise and additive correlated Gaussian white noise in the system process equations and observation equations. As can be seen from the actual motion trajectory, the motion is relatively violent, and big acceleration changes often occur, which results in rough motion curve and abundant burrs, showing a relatively extreme state of motion. In the case where both the system equation and the observation equation become inaccurate due to multiplicative noise, it can be seen that CKF has significantly decreased estimated performance, but still showing a tendency to track the actual trajectory movement. It can be seen from the figure that MACNCKF can still maintain very high tracking accuracy under non-ideal circumstance, which proves the correctness and superior performance of MACNCKF. The actual motion curve ends at the "T" point, and the CKF estimation curve ends at the "C" point, which are far from the actual position and thus unfavorable for navigation and positioning. The MACNCKF estimation curve in the figure ends at the "M" point, which almost coincides with the "T" point. For the convenience of observation, a partially enlarged view is added. It can be seen from the partially enlarged view that although the points "T" and "M" are not completely coincident, they are very close. On the one hand, it indicates that MACNCKF can deal with multiplicative noise and noise-related circumstances at the same time. On the other hand, it also suggests that there is room for improvement, which is worth further exploration.

To more accurately verify performance of the MACNCKF proposed herein, Figure 2 takes root mean square error (RMSE) of the estimation results of the two filters as the evaluation index.

It can be seen from Figure 2 that RMSE curve of CKF represented by the dashed line is much higher than that of MACNCKF represented by the solid line in Figures 2 (a)~2 (d), which proves superiority of MACNCKF in performance. CKF has higher accuracy and better numerical stability under ideal conditions than well-known nonlinear filters such as UKF and EKF. Nevertheless, it can be seen from the experimental results that under non-ideal conditions with the presence of multiplicative noise and additive-related noise, CKF performance is severely affected, indicating that CKF is inapplicable to such environments. CKF is essentially a kind of UKF, so we have done the same simulation for EKF as well, but the results of EKF diverge seriously, so it is not shown in the figure. However, the results show that EKF cannot effectively deal with the state estimation problem under such non ideal conditions. In addition, it can be seen from Figure 2 (c) and Figure 2 (d) that RMSE value of MACNCKF is quite small compared to that of CKF. It shows that MACNCKF can estimate the physical variable of velocity very accurately, which is very beneficial to improve motion performance of simulation object.

To verify the real-time performance of MACNCKF, we run CKF and MACNCKF 100,000 times in the presence of both multiplicative and correlated noise. The operation is conducted with CKF, MACNCKF, using a laptop with an Intel Core i5-9400F processor and 8GB RAM. We make Figure 3 based on data relationship in the experimental result.

This article has been accepted for publication in a future issue of this journal, but has not been fully edited. Content may change prior to final publication. Citation information: DOI 10.1109/ACCESS.2020.3021494, IEEE Access

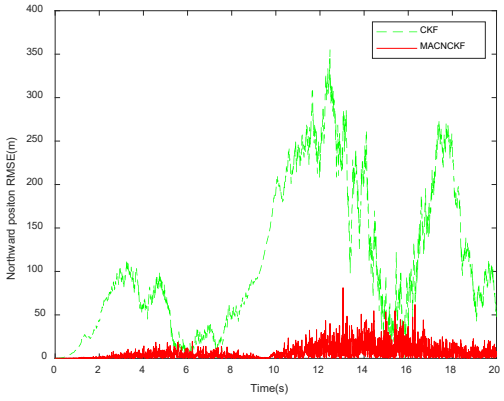

(a) Northward position RMSE

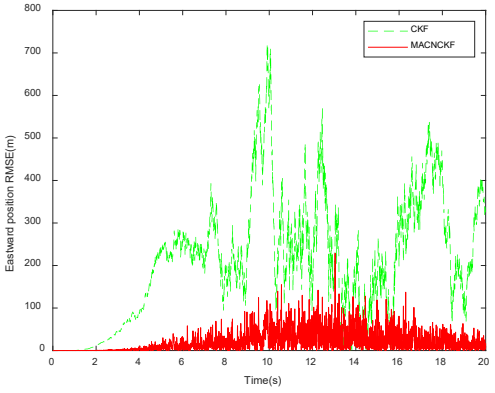

(b) Eastward position RMSE

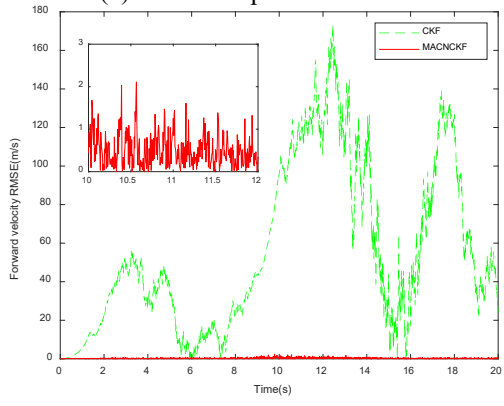

(c) Forward velocity RMSE

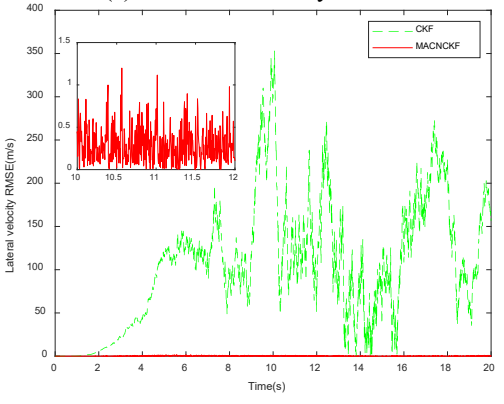

(d) Lateral velocity RMSE

FIGURE 2. Comparison of state estimation between CKF and MACNCKF of simulation object.

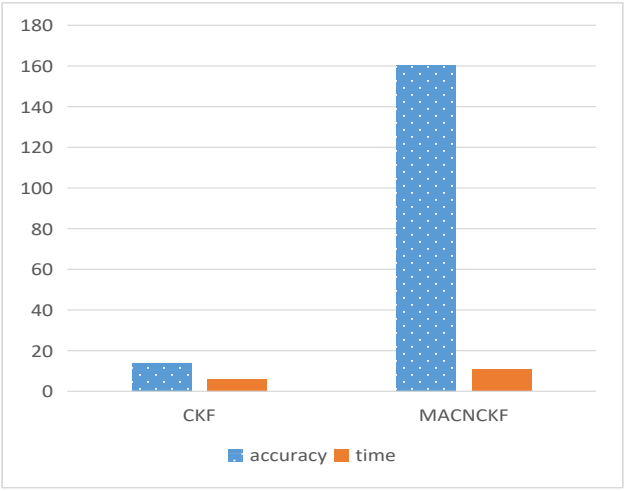

FIGURE 3. Comparison of two algorithms running 100000 times.

The results show that the average single run time of CKF is $6.1379e^{-5}s$, and the average single run time of MACNCKF is $1.0659e^{-4}s$, indicating that MACNCKF can fully meet real-time requirements of most systems. From Figure 3, it can be seen that MACNCKF has increased running time compared to CKF. This is because MACNCKF is an improved version based on CKF. However, the experimental results show that the time consumption is increased by less than one fold. The estimation accuracy is 11 times higher than that of CKF. It suggests that CKF has sharply decreased estimation accuracy and can hardly be used in such non-ideal environment, while MACNCKF completely overcomes this problem and guarantees the estimation performance.

5) VELOCITY ESTIMATION EXPERIMENT OF QUADRUPED ROBOT

The experimental prototype of the quadruped robot employed is shown in Figure 3. Robot body is equipped with power system consisting of engine, variable pump, and hydraulic accessories.

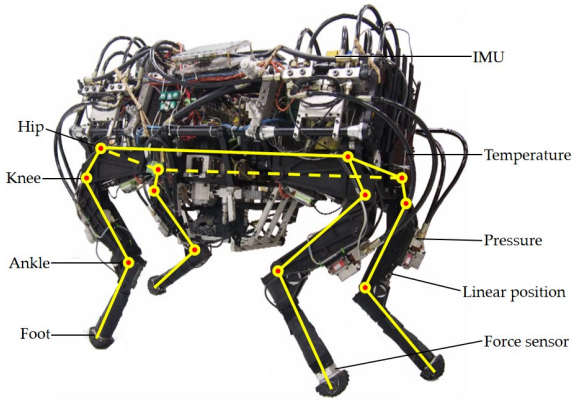

FIGURE 4. Platform of quadruped robot.

Since the magnitudes of these robotic parameters differ significantly from each other, the error values of displacement, velocity, accelerator bias are regarded as state variables, which can be expressed by equation (36):

So equation of state (37) can be rewritten as

$$x_{k+1} = F_k x_k + w_k \tag{49}$$

This article has been accepted for publication in a future issue of this journal, but has not been fully edited. Content may change prior to final publication. Citation information: DOI 10.1109/ACCESS.2020.3021494, IEEE Access

$$F_k = \begin{bmatrix} I & t & -\frac{T^2}{2}C_{b,k}^n \\ 0 & I & -TC_{b,k}^n \\ 0 & 0 & I \end{bmatrix} \tag{50}$$

$$w_k = \begin{bmatrix} -\frac{T^2}{2}C_{b,k}^n \Delta\delta_{a,k} \\ -TC_{b,k}^n \Delta\delta_{a,k} \\ \Delta\delta_{ba,k} \end{bmatrix} = \begin{bmatrix} -\frac{T^2}{2}C_{b,k}^n & 0 \\ -TC_{b,k}^n & 0 \\ 0 & I \end{bmatrix} \begin{bmatrix} \Delta\delta_{a,k} \\ \Delta\delta_{ba,k} \end{bmatrix} \tag{51}$$

In state variable $x_k = \begin{bmatrix} \Delta x_k & \Delta\dot{x}_k & \Delta b_{a,k} \end{bmatrix}^T$, Δx_k is the error value of displacement at the moment k, $\Delta\dot{x}_k$ is the error value of velocity at the moment k, $\Delta b_{a,k}$ is the error value of accelerator bias at the moment k. $\Delta\delta_{a,k}$ is the random error value of accelerator at the moment k and $\Delta\delta_{ba,k}$ is the random error value of accelerator bias at the moment k. C_b^n is rotation matrix, which is time-varying itself, so the process equation of the robot is also time-varying. IMU has a sampling frequency of 100HZ and a sensor sampling frequency of 200HZ, so $T = 0.005s$.

If the variance of $\Delta\delta_{a,k}$ is $Q_{a,k}$, the variance of $\Delta\delta_{ba,k}$ is $Q_{b,k}$, the process noise variance is

$$Q_k = E\left(\Delta\delta_{a,k}\Delta\delta_{a,k}^T\right) = \begin{bmatrix} \frac{t^4}{4}C_{b,k}^n C_{b,k}^{n\,T} Q_{a,k} & \frac{t^3}{2}C_{b,k}^n C_{b,k}^{n\,T} Q_{a,k} & 0 \\ \frac{t^3}{2}C_{b,k}^n C_{b,k}^{n\,T} Q_{a,k} & t^2 C_{b,k}^n C_{b,k}^{n\,T} Q_{a,k} & 0 \\ 0 & 0 & Q_{b,k} \end{bmatrix} \tag{52}$$

For the quadruped robot system, the observation equation is linearized. Based on this, MACNCKF needs only one volume point calculation for each filtering, which greatly reduces the calculation amount and improves real-time performance.

$$z_k = Hx_k + v_k \tag{53}$$

The above equation can be written as

$$z_k = \begin{bmatrix} I & 0 & 0 \\ 0 & I & 0 \end{bmatrix} \begin{bmatrix} \Delta x_k \\ \Delta\dot{x}_k \\ \Delta b_{a,k} \end{bmatrix} + v_k \tag{54}$$

For the quadruped robot system herein, $H \in R^{6\times 9}$, the observation noise covariance is

$$R_k = E\left(v_k v_k^T\right) \tag{55}$$

The obtained state estimate is an estimate of the error, which needs to be compensated to IMU for correction.

$$\begin{bmatrix} x_{c,k} \\ \dot{x}_{c,k} \\ a_{c,k} \end{bmatrix} = \begin{bmatrix} x_{i,k} \\ \dot{x}_{i,k} \\ a_{i,k} \end{bmatrix} - \begin{bmatrix} \Delta\hat{x}_k \\ \Delta\hat{\dot{x}}_k \\ C_{b,k}^n \Delta\hat{b}_{a,k} \end{bmatrix} \tag{56}$$

where $x_{i,k}$, $\dot{x}_{i,k}$ and $a_{i,k}$ are navigation calculation results at the moment k. $\Delta\hat{x}_k$, $\Delta\hat{\dot{x}}_k$ and $\Delta\hat{b}_{a,k}$ are estimations of displacement and velocity errors at the moment k. $x_{c,k}$, $\dot{x}_{c,k}$ and $a_{c,k}$ are position, velocity, and acceleration results of the robot in the navigation coordinate system after correction at the moment k. Figure 5 is a video screenshot of a quadruped robot walking in place with MACNCKF. It can be seen from Figure 5 that the quadruped robot steps in the trot gait. When a pair of diagonal legs are in a stable supporting state, the robot mass center does not move significantly, and then it alternates to another pair of diagonal legs as supporting legs. The whole process is smooth and stable. The correctness and validity of MACNCKF are testified by experiments.

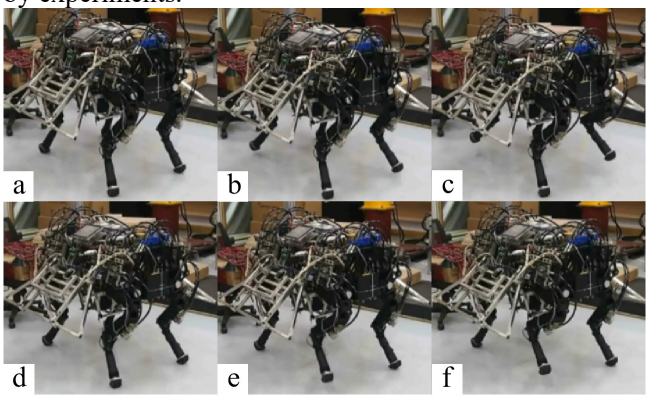

FIGURE 5. A screenshot of a quadruped robot walking in place. (a) The robot is ready to start a new trot gait cycle; (b) The robot raises the left front leg and right hind leg on the diagonal line; (c) The left front leg and right hind leg of the robot are lifted to the highest point, and the robot chooses landing points according to the self motion state estimated by the state; (d) The left front leg and right hind leg of the robot are placed on the selected landing points to maintain balance and original state; (e) The robot lifts the right front leg and left hind leg on the diagonal line; (f) The right front leg and left hind leg of the robot are lifted to the highest point, and the landing points are selected according to the self motion state estimated by the state to maintain the balance and original state.

This experiment will verify MACNCKF effectiveness in practical system application and its applicability in time-varying systems. In fact, for a system with multiplicative noise, there is almost no time-invariant system. After polluting the original time-invariant system with multiplicative noise, the system becomes time-varying as multiplicative noise is time-varying. If this case is not detected in time, there will be unexpected results. The quadruped robot is a time-varying system as it introduces a rotation matrix in the modeling. Due to random uncertainties of the system model parameters caused by modeling errors, model simplification, random interference, and body buffet, it is very susceptible to multiplicative noise pollution. The same working environment makes additive noise no longer satisfy the hypothesis of mutual independence, so the application on quadruped robots seems very appropriate. Experimental noise variance and correlation, multiplicative noise mean and covariance of related additive noise can be statistically approximated by wavelet filtering and Allan

This article has been accepted for publication in a future issue of this journal, but has not been fully edited. Content may change prior to final publication. Citation information: DOI 10.1109/ACCESS.2020.3021494, IEEE Access

variance. Based on the information collected by the linear displacement sensors of the quadruped robot's legs, forward kinematics is calculated. The landing leg is determined using sole force sensor to further improve accuracy of the solution. The fusion estimation of the solution results with the IMU through CKF or MACNCKF is carried out to obtain more accurate results for robot control and navigation. The process is complicated and beyond the research content of this paper, which will not be discussed here. As the dynamic capture system cannot be used, the robot performs in-situ stepping in the experiment to ensure that the true value is easier to determine, and the experimental results are more clear and readable. The system is initialized for 10 seconds in the experiment, and then remains stationary, and in-situ stepping starts at 28th second and stops after 12 seconds. The result is shown in Figure 6.

As can be seen from Figure 5, the dashed line represents CKF estimation curve, and the solid line represents MACNCKF estimation curve. Considering the great overlapping parts of the curve, dotted line, solid line and a partially enlarged view are used for the convenience of observation. Figure 5 (a) represents the northward position of the robot in the world coordinate system; Figure 5 (b) represents the forward speed of the robot in the proprio-coordinate system, with the forward direction being positive. Figure 5 (c) represents the eastward position of the robot in the world coordinate system; Figure 5(d) represents the lateral speed of the robot in the proprio-coordinate system, with the right direction being positive. To avoid ambiguity, the robot is oriented to the north in the experiment. The robot steps well on the spot and basically remained in situ. It can be seen from Figure 5(a) that the MACNCKF estimation curve shows only a slight movement. A slight northward movement can be seen in the partially enlarged view, which is consistent with the reality, demonstrating accuracy of MACNCKF. However, CKF estimation curve indicates that the robot reciprocates within a range of 5 meters, which is inconsistent with actual observation. Such an estimation error is very serious, which is unfavorable for robot control and navigation. The accuracy of CKF itself can reach the third-order accuracy of Taylor series expansion. The reason for such a big error is that the working environment of the quadruped robot does not meet the basic hypothesis of Kalman filtering. It can be seen from MACNCKF curve in Figure 5(b) that the forward velocity of the robot has been alternated between $-1m/s \sim 1m/s$, which is caused by in-situ step control of the balance and accords with the control algorithm. Moreover, it is found from the partially enlarged diagram that MACNCKF velocity estimation waveform has greater pulse width in the positive direction than in the negative direction, making displacement after the velocity integration positive, which also verifies the observation that the robot moves slightly in a positive direction in Fig. 5(a). As a result, the correctness and accuracy of MACNCKF are further verified. The velocity estimation curve of CKF has great fluctuations, and the subsequent velocity estimation curve returns to zero more slowly than MACNCKF. Moreover, such estimation error will result in serious misjudgment of its own motion state by the robot, causing damage to the system security. It can be seen from Figure 5(c) that the MACNCKF eastward position estimation curve displays a slight east-west swing in the robot, which is related to orientation of the robot in the experiment. Since the robot is artificially oriented north, Figure 5(c) approximates the robot's lateral position. After the system initialization, MACNCKF's eastward estimated value shows an eastward shift of 3.6mm in the robot, so the robot slowly autonomously adjusts the position westward. The partially enlarged view shows that with a slight swing, the robot moves slightly to the west, and the eastward position curve basically returns to zero when the step is stopped. It indicates that MACNCKF cooperates with the quadruped robot to achieve superior autonomous control. The eastward position estimation curve of CKF has big amplitude, which shows that MACNCKF has achieved precise control of the robot. Since the IMU can continue to work after the robot terminates the controller, it is observed that the robot deviated 2.6mm westward after 57s. Since the position and velocity of the robot in the vertical direction are not recorded, this westward displacement may be caused by body tilt after loss of control, which may be related to the gap during processing and installation. This normal phenomenon will not affect the experimental results. It can be seen clearly from the MACNCKF lateral velocity estimation curve in Figure 5(d) that during autonomous robot adjustment, the body makes slight adjustment to maintain balance. These small details are accurately and clearly captured by MACNCKF via lateral velocity estimation curve, verifying accuracy and reliability of MACNCKF. It can be seen from the partially enlarged view that during the stepping phase, the velocity is biased to a negative value, that is, the left side of the body is westward during the experiment, which is consistent with the direction of motion adjustment in Figure 5(c). However, CKF lateral velocity estimation curve in the partially enlarged view not only features big amplitude, but also lacks obvious directivity. The above experimental results indicate that MACNCKF has good estimation accuracy and convergence velocity in practical applications, and can effectively solve state estimation problems involving both multiplicative and additive noise. It also suggests that although CKF demonstrates good estimation performance under ideal conditions, the estimation performance will drop sharply under non-ideal conditions, with lower estimation accuracy and convergence velocity compared to MACNCKF. The estimation result of CKF has bigger error and slower convergence velocity compared to that of MACNCKF. It can also be seen from the experimental results that the CKF estimation curve has big amplitude, which may be due to the robot's buffet itself. However, it can also be seen that such

This article has been accepted for publication in a future issue of this journal, but has not been fully edited. Content may change prior to final publication. Citation information: DOI 10.1109/ACCESS.2020.3021494, IEEE Access

buffet has a small impact on MACNCKF and MACNCKF can well isolate such interference.

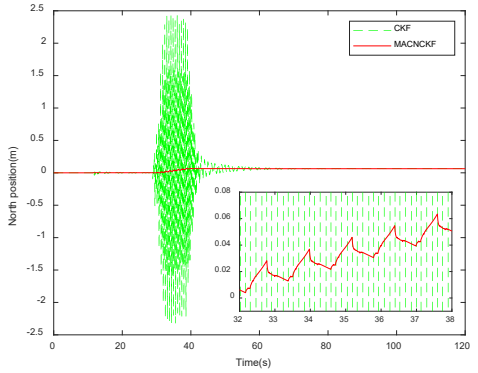

(a) North position

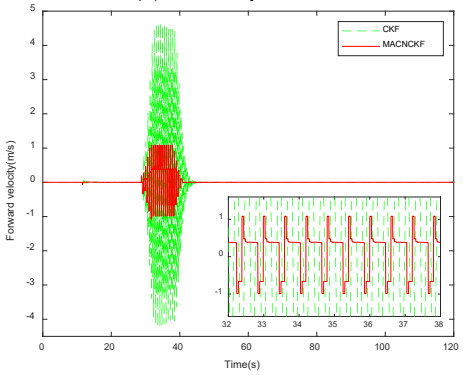

(b) Forward velocity

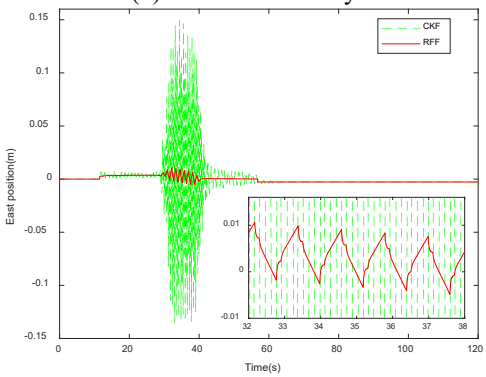

(c) East position

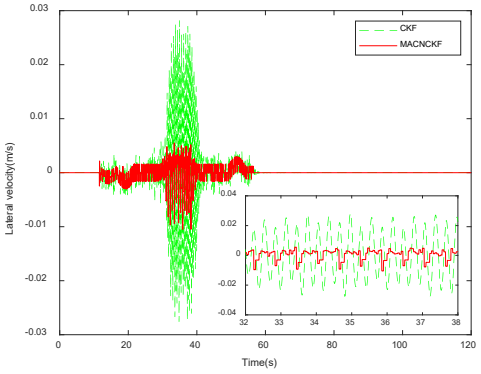

(d) Lateral velocity

FIGURE 6. Comparison of state estimation between CKF and MACNCKF of a quadruped robot.

III. CONCLUSION

In this paper, MACNCKF is proposed to solve the state estimation problem involving both multiplicative and additive noise. While maintaining the advantages of CKF algorithm, it overcomes hypothetical limitation of KF. MACNCKF can be easily and conveniently transplanted into various derived filters of CKF. When multiplicative noise and additive noise are independent of each other, MACNCKF is degraded to corresponding filter in a general form, which extends application scope of CKF series filter, thus improving robustness and reliability of the filter. The entire algorithm has undergone strict mathematical derivation, and its correctness and real-time performance have been verified through simulation experiments. The application of MACNCKF in quadruped robot system further verifies its accuracy, feasibility and reliability. The above results demonstrate that MACNCKF has superior estimation performance and can effectively solve state estimation issues involving both multiplicative and additive noise.

REFERENCES

[1] T.D. Barfoot, "State Estimation for Robotics,", Cambridge: Cambridge University Press, 2017.

[2] Y. Bar-ShalomX.R. Li and T. Kirubarajan, "Estimation with applications to tracking and navigation: theory algorithms and software,",John Wiley & Sons, 2004.

[3] S.J. Julier and J.K. Uhlmann, "Unscented filtering and nonlinear estimation," *P. Ieee*, vol. 92, no. 3, pp. 401-422, 2004.

[4] I. Arasaratnam and S. Haykin, "Cubature kalman filters," *IEEE T. Automat. Contr.*, vol. 54, no. 6, pp. 1254-1269, 2009.

[5] J. Won, J. Park, K. Park, H. Yoon and D. Moon, "Non-Target Structural Displacement Measurement Using Reference Frame-Based Deepflow," *Sensors-Basel*, vol. 19, no. 13, pp. 2992, 2019.

[6] M. Morshidi and T. Tjahjadi, "Gravity optimised particle filter for hand tracking," *Pattern Recogn.*, vol. 47, no. 1, pp. 194-207, 2014.

[7] S. Guo, S. Pan, L. Shi, P. Guo, Y. He and K. Tang, "Visual detection and tracking system for a spherical amphibious robot," *Sensors-Basel*, vol. 17, no. 4, pp. 870, 2017.

[8] H. Zhang, J. Xie, J. Ge, W. Lu and B. Liu, "Strong tracking SCKF based on adaptive CS model for manoeuvring aircraft tracking," *IET Radar, Sonar & Navigation*, vol. 12, no. 7, pp. 742-749, 2018.

[9] Q. ZhenbingQ. Huaming and W. Guoqing, "Adaptive robust cubature Kalman filtering for satellite attitude estimation," *Chinese J. Aeronaut.*, vol. 31, no. 4, pp. 806-819, 2018.

[10] B. KangK. Chong and D. Lee, "Precise Indoor Positioning Algorithms for Autonomous Hexa-Rotor Using Cubature Kalman Filter," *Advanced Science Letters*, vol. 21, no. 10, pp. 2993-2996,

This article has been accepted for publication in a future issue of this journal, but has not been fully edited. Content may change prior to final publication. Citation information: DOI 10.1109/ACCESS.2020.3021494, IEEE Access

2015.
[11] X. HuY. Hu and B. Xu, "Generalised Kalman filter tracking with multiplicative measurement noise in a wireless sensor network," *IET Signal Process.*, vol. 8, no. 5, pp. 467-474, 2013.
[12] W. LiuX. Wang and Z. Deng, "Robust Kalman estimators for systems with mixed uncertainties," *Optimal Control Applications and Methods*, vol. 39, no. 2, pp. 735-756, 2018.
[13] W. LiuX. Wang and Z. Deng, "Robust Kalman estimators for systems with multiplicative and uncertain-variance linearly correlated additive white noises," *Aerosp. Sci. Technol.*, vol. 72, pp. 230-247, 2018.
[14] W. LiuX. Wang and Z. Deng, "Robust centralized and weighted measurement fusion Kalman predictors with multiplicative noises, uncertain noise variances, and missing measurements," *Circuits, Systems, and Signal Processing*, vol. 37, no. 2, pp. 770-809, 2018.
[15] W.Q. LiuX.M. Wang and Z.L. Deng, "Robust centralized and weighted measurement fusion white noise deconvolution estimators for multisensor systems with mixed uncertainties," *Int. J. Adapt. Control*, vol. 32, no. 1, pp. 185-212, 2018.
[16] C. YangZ. Yang and Z. Deng, "Robust weighted state fusion Kalman estimators for networked systems with mixed uncertainties," *Inform. Fusion*, vol. 45, pp. 246-265, 2019.
[17] X. WangW. Liu and Z. Deng, "Robust weighted fusion Kalman estimators for multi-model multisensor systems with uncertain-variance multiplicative and linearly correlated additive white noises," *Signal Process.*, vol. 137, pp. 339-355, 2017.
[18] X. WangW. Liu and Z. Deng, "Robust weighted fusion Kalman estimators for systems with multiplicative noises, missing measurements and uncertain-variance linearly correlated white noises," *Aerosp. Sci. Technol.*, vol. 68, pp. 331-344, 2017.
[19] G. Chang, "Marginal unscented Kalman filter for cross-correlated process and observation noise at the same epoch," *IET Radar, Sonar & Navigation*, vol. 8, no. 1, pp. 54-64, 2014.
[20] D. Simon, "Optimal state estimation: Kalman, H infinity, and nonlinear approaches,",John Wiley & Sons, 2006.
[21] S. Saha and F. Gustafsson, "Particle filtering with dependent noise processes," *IEEE T. Signal Proces.*, vol. 60, no. 9, pp. 4497-4508, 2012.
[22] X. WangM. Fu and H. Zhang, "Target tracking in wireless sensor networks based on the combination of KF and MLE using distance measurements," *IEEE T. Mobile Comput.*, vol. 11, no. 4, pp. 567-576, 2011.
[23] M.V. Basin, "Root-mean-square filtering of the state of polynomial stochastic systems with multiplicative noise," *Automat. Rem. Contr.+*, vol. 77, no. 2, pp. 242-260, 2016.
[24] S. Wang, Y. Feng, S. Duan and L. Wang, "Mixed-Degree Spherical Simplex-Radial Cubature Kalman Filter," *Math. Probl. Eng.*, vol. 2017, 2017.
[25] Y. Zhang, Y. Huang, Z. Wu and N. Li, Seventh-degree spherical simplex-radial cubature Kalman filter, IEEE, 2014, pp. 2513-2517.

JIKAI LIU was born in Harbin, Heilongjiang, China. He is a doctor of mechanical engineering in Harbin Institute of Technology at present, and he is a Reviewer of IEEE ACCESS as well.

He has participated in a number of NSFC projects. His main research fields are bionic robot, state estimation, machine vision and artificial intelligence.

PENGFEI WANG studies bionics and intelligent robots. He received the Ph.D. degree in mechanical engineering from Harbin Institute of Technology, in 2007.

He was a Research Assistant in Harbin Institute of Technology from 2007 to 2011. Since 2011, he has been an Assistant Professor . He has a good command of intelligent robot, industrial robot, military robot, Micro robot system, multi legged bionic robot system, bionic control, crawler type reconfigurable micro robot, micro acoustic anti-terrorism wall climbing robot, etc.

MANTIAN LI mainly studies bionics and intelligent robots. He received the Ph.D. degree in mechanical engineering from Harbin Institute of Technology, in 2006.

From 2004 to 2008, he was a Research Assistant . Since 2008, he has been an Assistant Professor in Institute of robotics, Harbin Institute of Technology. He is good at Micro robot system, multi legged bionic robot system, bionic control, crawler type reconfigurable micro robot, micro acoustic anti-terrorism wall climbing robot, intelligent robot, industrial robot, military robot, etc.

This article has been accepted for publication in a future issue of this journal, but has not been fully edited. Content may change prior to final publication. Citation information: DOI 10.1109/ACCESS.2020.3021494, IEEE Access

WEI GUO mainly studies bionic robot and bionic control. She received her doctorate in mechanical engineering from Harbin Institute of Technology in 2002. Since 2013, she has been a Professor and Doctoral Supervisor in Institute of robotics, Harbin Institute of Technology.

Her main research direction is special mobile robot technology, bionic robot and bionic control, bionic robot technology and artificial intelligence. She has carried out in-depth research and achieved important results in the aspects of special micro and bionic robot system technology, advanced robot control theory and method.

FUSHENG ZHA mainly studies bionics and intelligent robots. He received his doctorate in mechanical engineering from Harbin Institute of Technology in 2012.

From December 2016 to present, he has been an Assistant Professor, Doctoral Supervisor in Institute of robotics, Harbin Institute of Technology. His main research directions are artificial intelligence, vision, mobile operation and legged robot. In recent five years, he has published 18 SCI articles and 33 EI articles and obtained three scientific research awards.

LINING SUN is mainly engaged in the research and development of robots. He received his doctorate in mechanical engineering from Harbin Institute of Technology in 1993.

From 1998 to 2008, he was a former Director of Institute of robotics, Harbin Institute of Technology. Since 2007, he has been Deputy Director of State Key Laboratory of robotics and systems. He also serves as Vice President of micro nano device and system technology branch of China Instrument and instrument society, Chairman of micro nano robot branch of China micro nano society, Director of medical robot branch of China Medical Device Industry Association, Vice President of China Mechatronics Technology Application Association, and Deputy Director of robot Committee of China Society of automation.

Prof. Sun has a good command of industrial robots and electromechanical integration equipment, micro nano operation robots and equipment, medical and special robots, etc., and has obtained important research results in the research and application of advanced robot mechanism, perception, control, system integration and other frontier and core key technologies.

PENGLONG ZHENG received his master degree in mechatronics engineering from Harbin Institute of Technology in 2018, and is now a Ph.D. student working on the control theory and system dynamics of the underactuated quadruped robot. His aim is to build a robust, agility and high-speed robot.